Micromechanical analysis on transverse compressive behavior and damage mechanism of CF/Al composites considering realistic fiber-arrangement

Zhenjun Wang[1], Zhongyuan Wang[1], Jinqiu Zhou[2], Changchun Cai[1], Bowen Xiong[1], Wei Yang[1], Siyuan Yang[1], and Aodi Zhang[1]

[1]Nanchang Hangkong University
[2]Commercial Aircraft Corporation of China Ltd

April 28, 2020

Abstract

A micromechanical model based on the realistic microstructure of carbon fiber reinforced aluminum (CF/Al) composites was developed for the first time. The transverse compressive behaviors, with particular emphasis on damage mechanism of the composites were investigated by numerical simulation and experiment. The results showed that the micromechanical model considering the realistic fiber arrangement predicts the mechanical properties more accurately than that based on an idealized fiber arrangement, and the calculated stress-strain curves agrees well with the experimental ones. The interfacial damage accumulates with compressive strain increasing, and induces the local interface failure successively. The progression and interaction of interface failure and matrix damage dominates the transverse compression process, and leads to the initiation of fiber failure in the ultimate stage, resulting in a fracture surface with the characteristic of interfacial debonding and fiber rupture. Moreover, parametric analysis based on the micromechanics model was carried out to evaluate the influences of interfacial properties and fiber volume fraction on the transverse compressive behavior of the composites.

Hosted file

`Manuscript.docx` available at https://authorea.com/users/311004/articles/441759-micromechanical-analysis-on-transverse-compressive-behavior-and-damage-mechanism-of-cf-al-composites-considering-realistic-fiber-arrangement

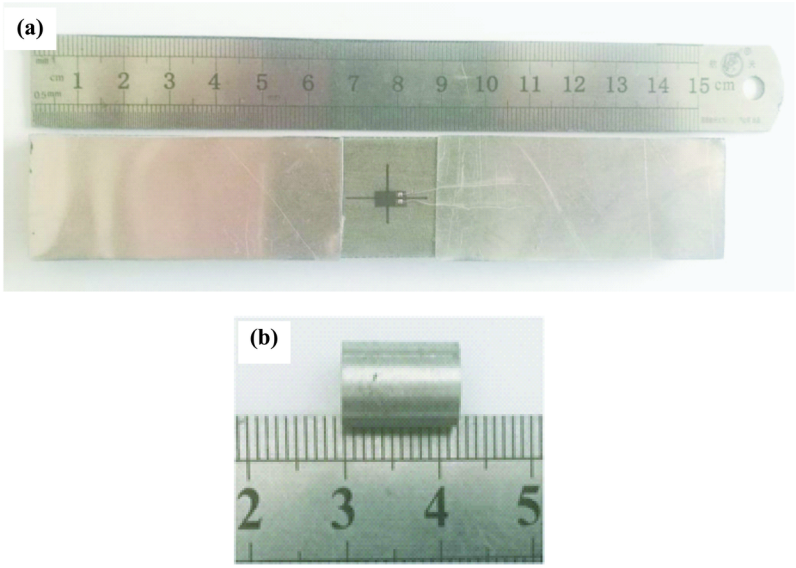

Fig.1 Sample of the CF/Al composite (a) and the ZL301 alloy (b) for uniaxial compression testing

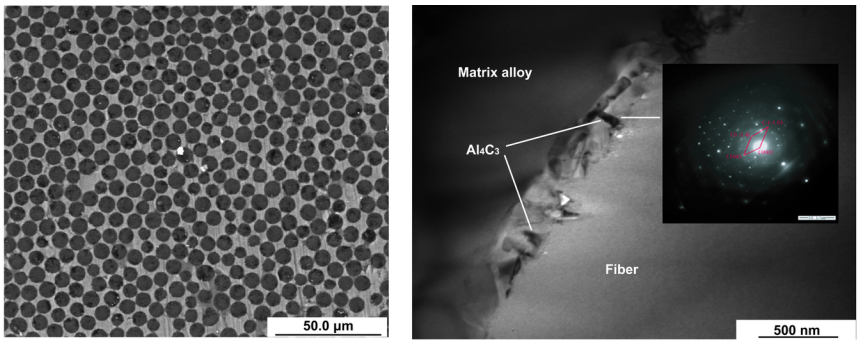

Fig.2 Microstructure of the CF/Al composite (SEM) (a) and the matrix/fiber interface (TEM) in the composite (b). The inset in Figure 2b is the SAED pattern of the interfacial product

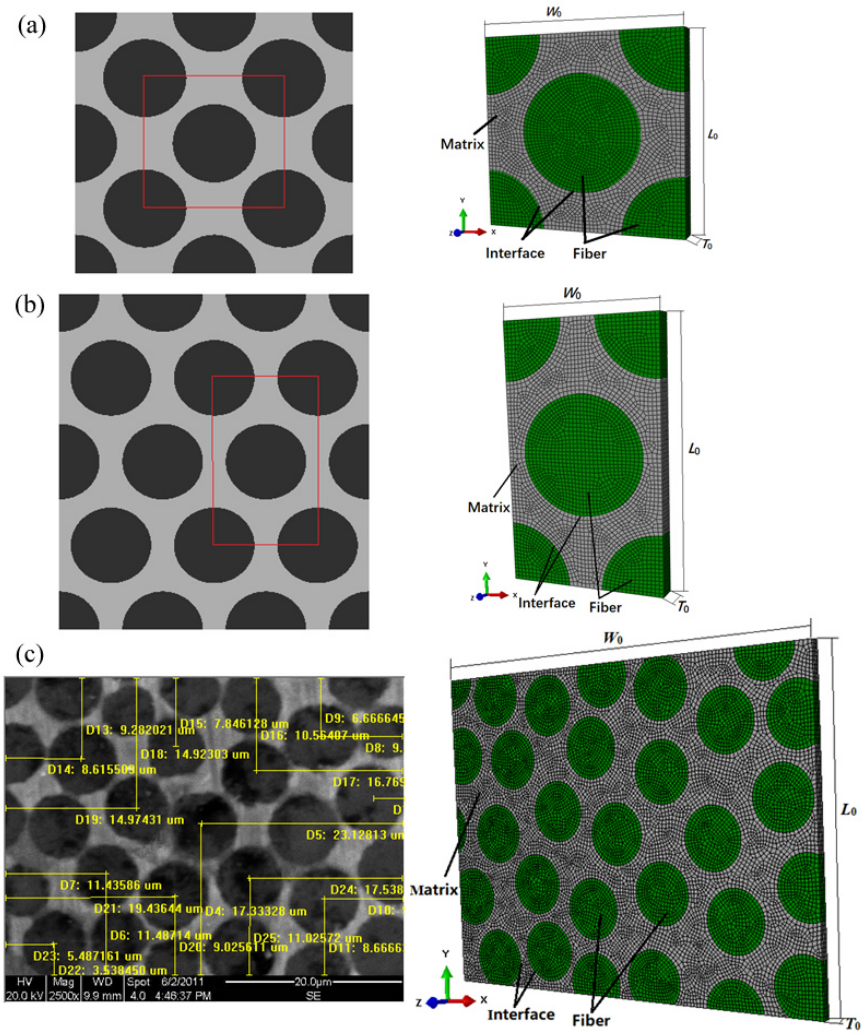

Fig.3 RVE models with the idealized and realistic fiber array geometries
(a) S-RVE model, (b) H-RVE model, and (c) R-RVE model

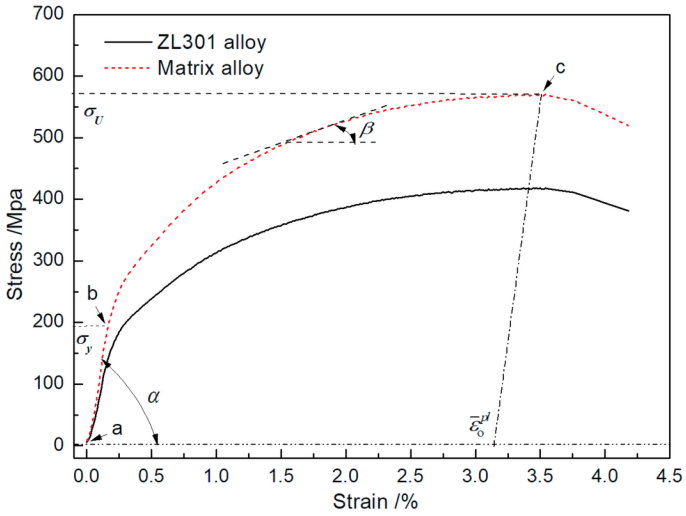

Fig.4 Experimental stress-strain curve of the ZL301 alloy and in-situ compressive curve of the matrix alloy

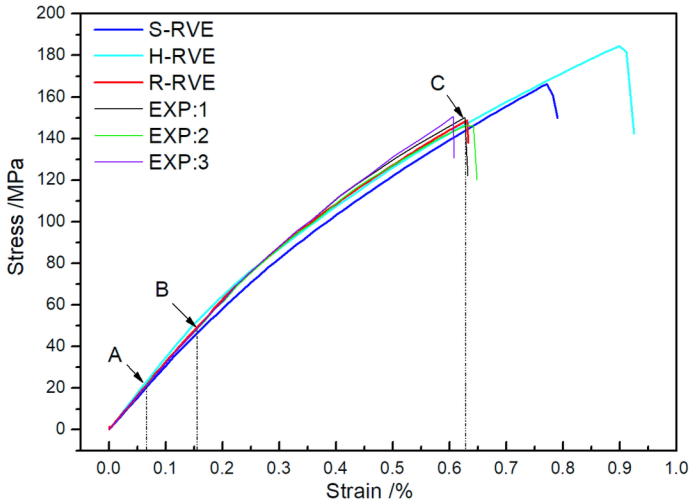

Fig.5 Comparison of transverse compression stress-strain curves for the CF/Al composites: Testing curves and predicted curves by the different RVE models

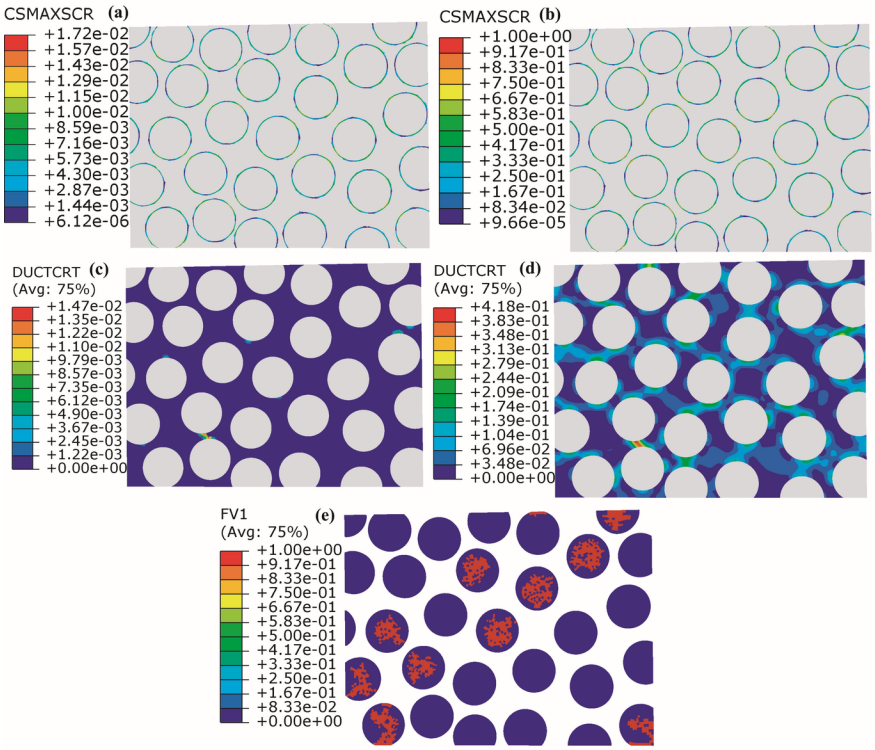

Fig.6 Microscopic damage and failure behaviors of the constituents during transverse compression process: (a)Interfacial damage (ε=0.001%), (b)Interfacial failure (ε=0.066%), (c)Matrix damage (ε=0.152%), (d)Matrix damage (ε=0.630%), (e)Fiber failure (ε=0.630%)

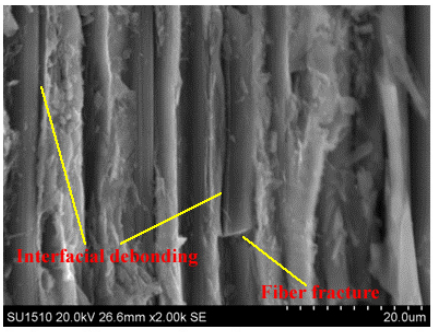

Fig.7 Fracture morphology of the composite under transverse compression condition (SEM)

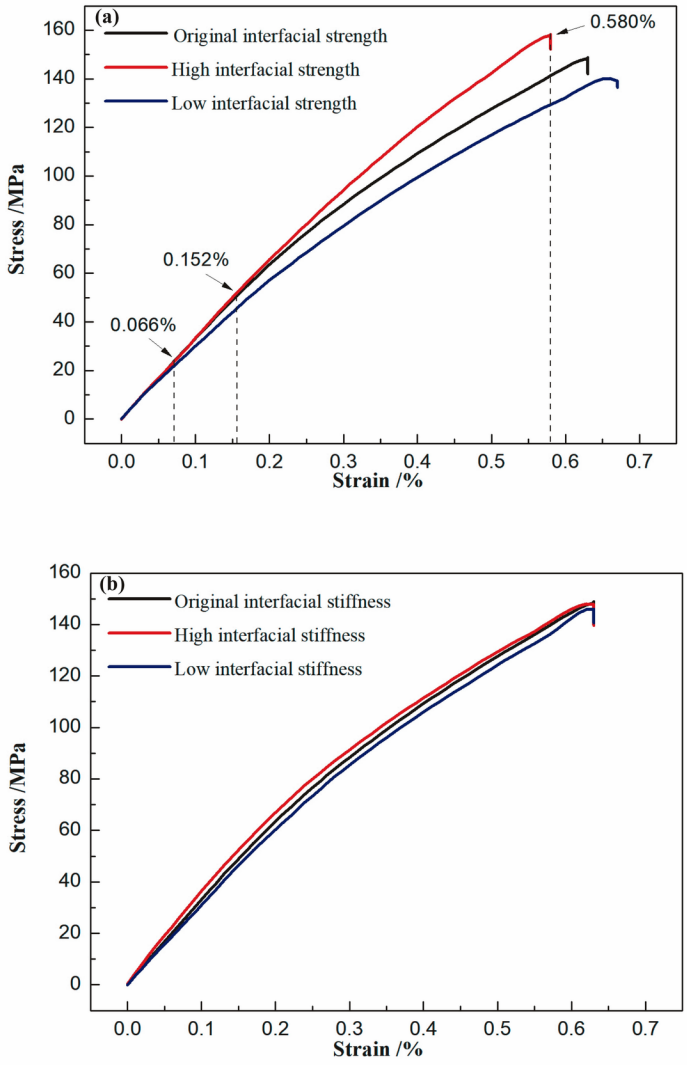

Fig.8 Effect of interfacial strength (a) and interfacial stiffness (b) on the transverse compressive stress-strain behaviors

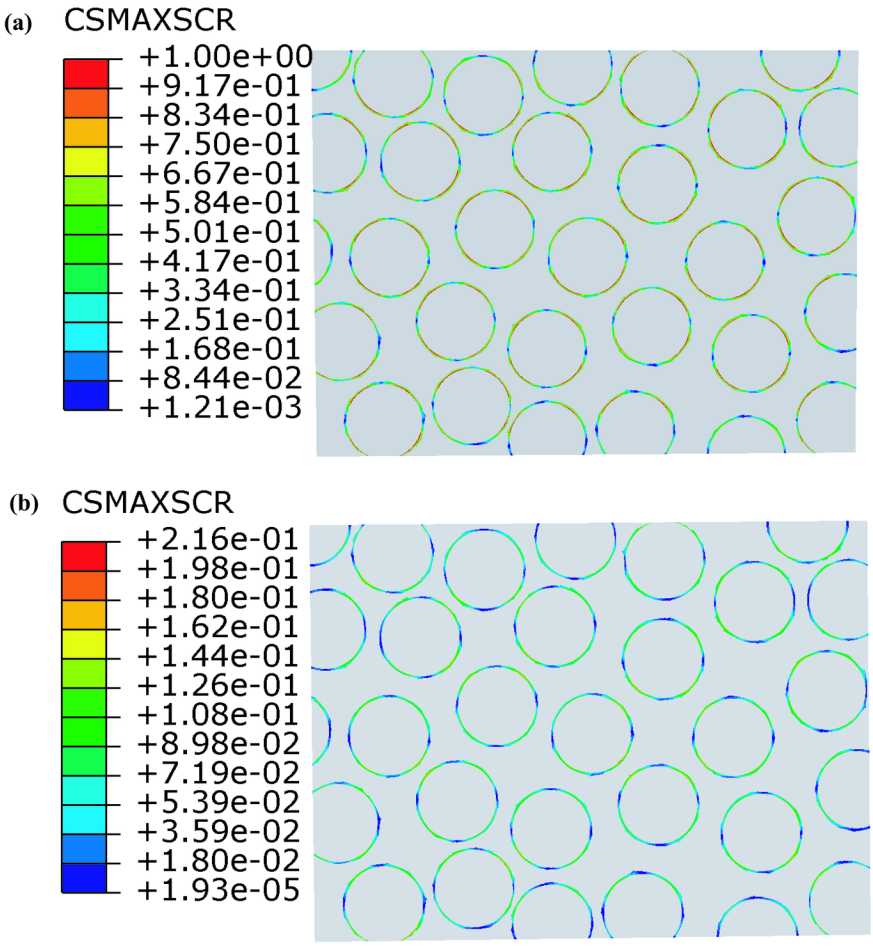

Fig.9 Interfacial damage state at ε=0.066%: (a) the low interfacial strength, (b) the high interfacial strength

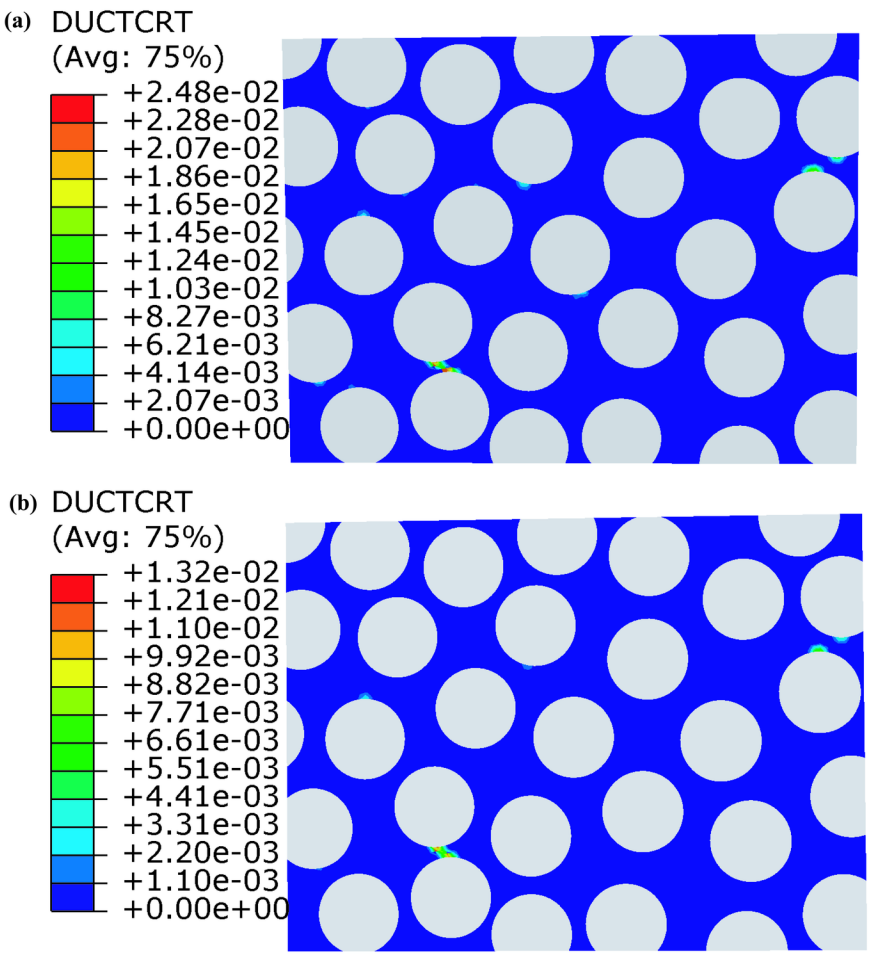

Fig.10 Damage state of the matrix alloy at ε=0.152%: (a) the low interfacial strength, (b) the high interfacial strength

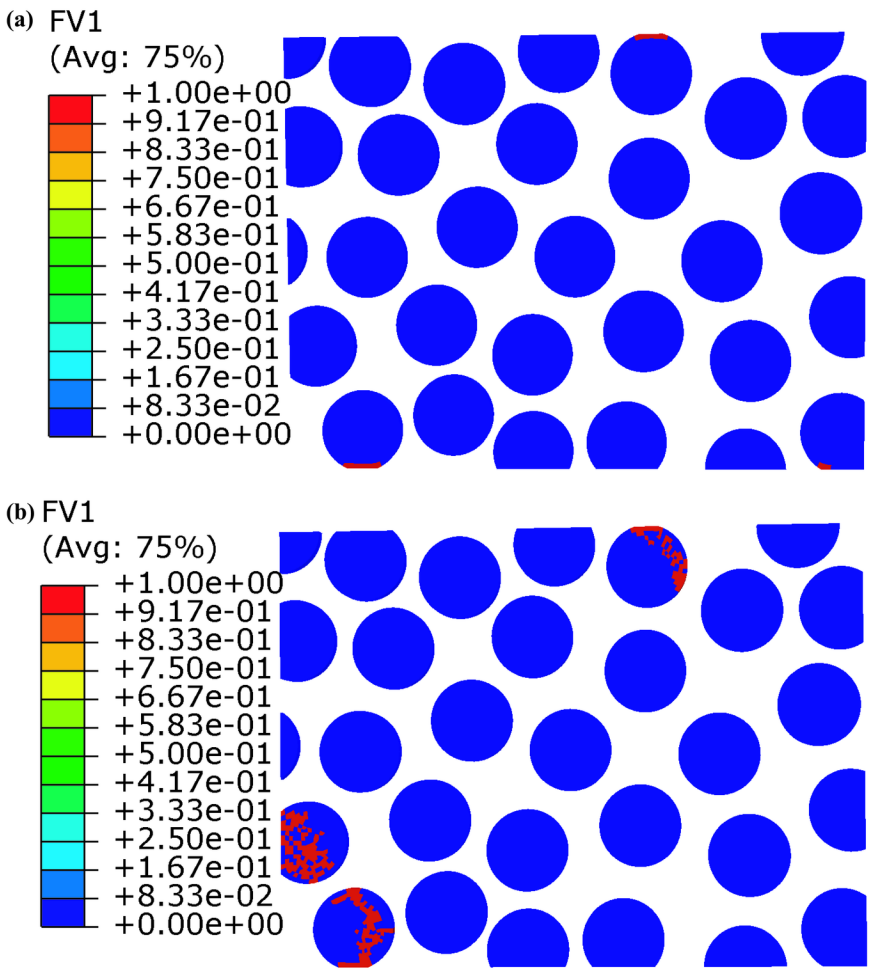

Fig.11 Failure state of the fibers at ε=0.580%: (a) the low interfacial strength, (b) the high interfacial strength

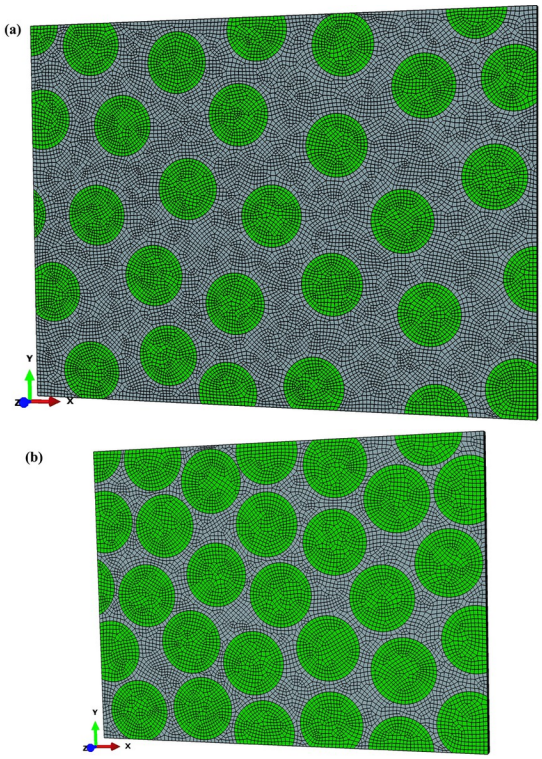

Fig.12 RVE models with fiber volume fraction: (a) $V_f = 40\%$ and (b) $V_f = 70\%$

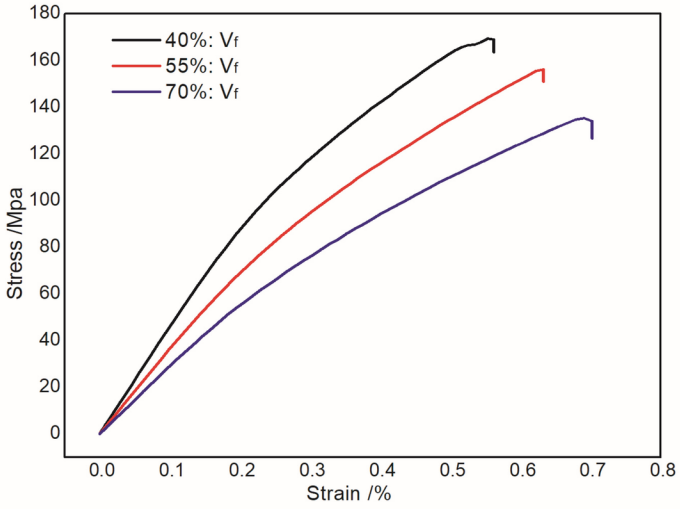

Fig.13 Transverse compressive curves at the different fiber volume fraction conditions

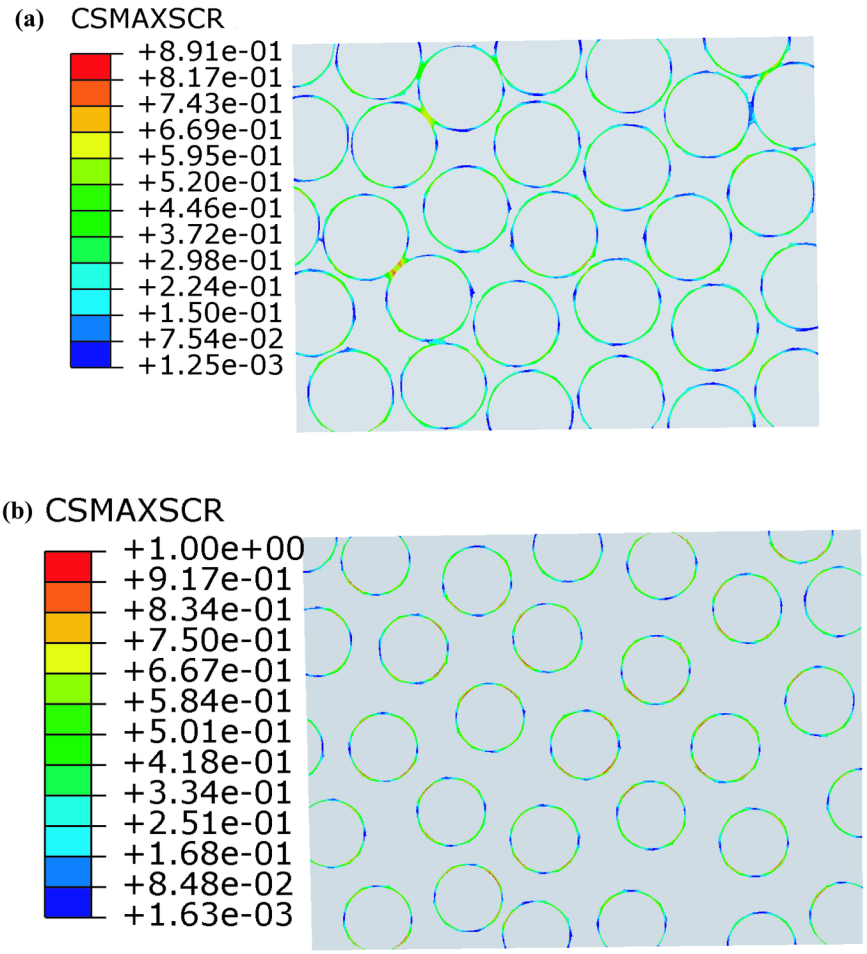

Fig.14 Interfacial damage state (ε=0.066%) at the V_f=70% (a) and the V_f=40% (b) conditions

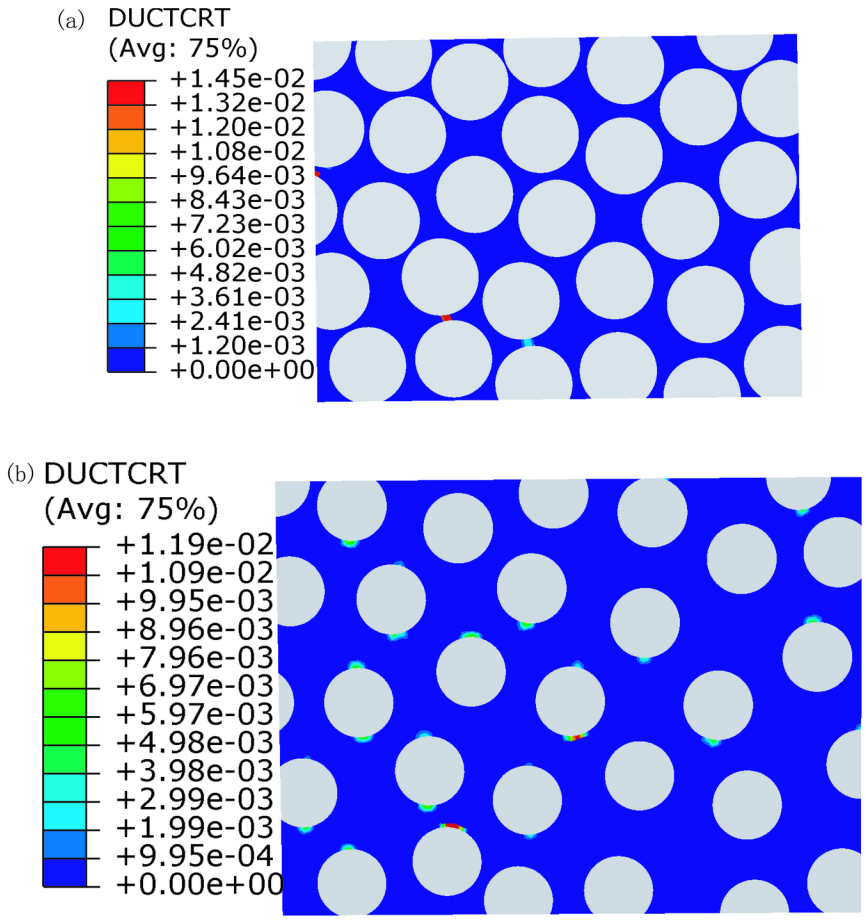

Fig.15 Matrix damage state (ε=0.152%) at the V_f=70% (a) and the V_f=40% (b) conditions

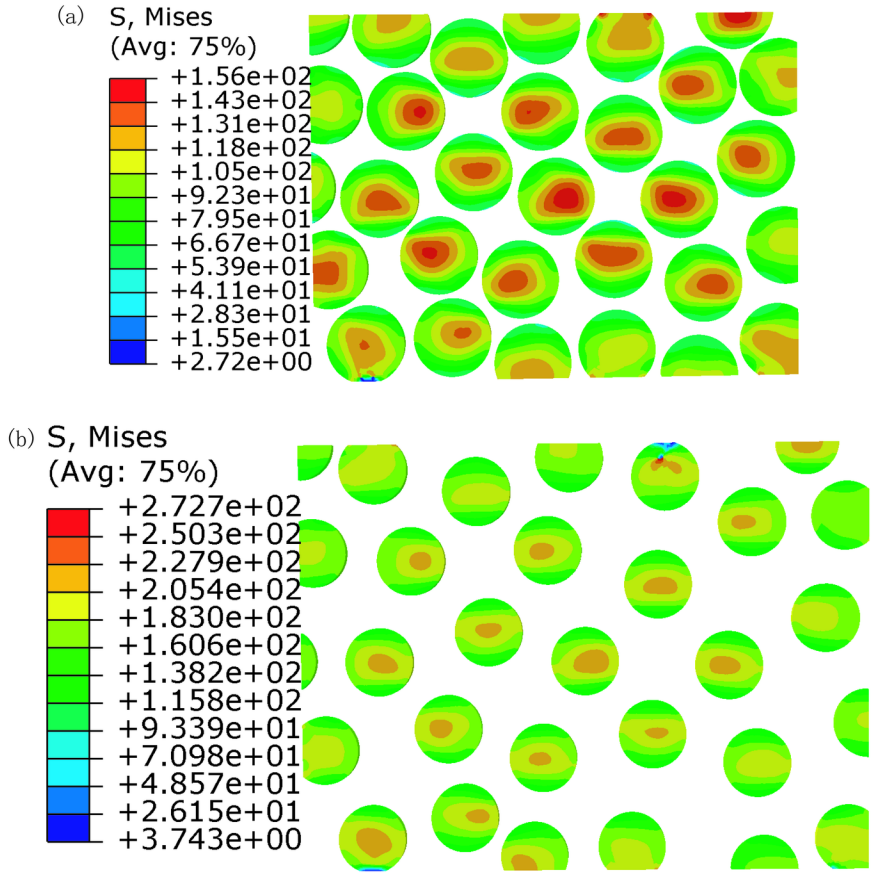

Fig.16 Stress contours of fibers (ε=0.500%) at the V_f=70% (a) and the V_f=40% (b) conditions